MedChemComm

The official journal of the European Federation for Medicinal Chemistry

Accepted Manuscript

This article can be cited before page numbers have been issued, to do this please use: F. Yang, D. Ge, L. Han, Y. Yang, Y. Chen, H. Zhang and N. Zhao, *Med. Chem. Commun.*, 2019, DOI: 10.1039/C9MD00306A.

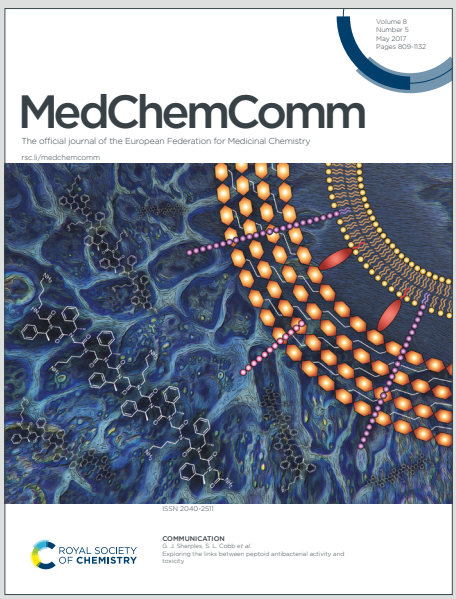

ROYAL SOCIETY OF CHEMISTRY

rsc.li/medchemcomm

View Article Online
DOI: 10.1039/C9MD00306A

ARTICLE

Development of Hydroxamate-Based Histone Deacetylase Inhibitors of Bis-substituted Aromatic Amides with Antitumor Activities

Received 00th January 20xx,
Accepted 00th January 20xx

DOI: 10.1039/x0xx00000x

Di Ge,[1,#] Lina Han,[1,#] Feifei Yang,[1,2,#,*] Na Zhao, Yang Yang,[2] Hua Zhang,[1,*] and Yihua Chen[2,*]

Previously, we designed and synthesized a series of bis-substituted aromatic amide-based histone deacetylase (HDAC) inhibitors. In this study, we report the replacement of bromine atom by different amides on the phenyl ring of the CAP region. Representative compounds **9d** and **10k** exhibited low nanomolar IC_{50}s against HDAC1, which were ten times lower than the positive control SAHA. The IC_{50} of **9d** against human A549 cancer cell line was 2.13 μM. Furthermore, **9d** increased the acetylation of histone H3 and H4 in a dose-dependent manner. Moreover, **9d** significantly arrested A549 cells at G2/M phase and induced A549 cells apoptosis. Finally, molecular docking investigation rationalized the high potency of compound **9d**.

1. Introduction

Epigenetic modification plays an important role in the treatment of cancers[1,2]. Protein lysine acetylation, regulated by histone acetyltransferases (HATs) and histone deacetylases (HDACs), can lead to changes in gene expression without modifying the gene sequence[3,4]. HATs neutralize the positive charge of lysine residues by adding an acetyl group to the *N*-terminal tail of histone, which results in open and transcriptionally active chromatin structure. Contrarily, HDACs remove the acetyl group, leading to closed chromatin structure and transcriptional repression[5,6]. The overexpression of HDACs has been found in various cancers, which is associated with the down-regulation expression of onco-suppressor genes[7]. Meanwhile, some non-histone proteins such as tubulin, HSP90, p53 and ER, also serve as substrates of HDACs[8-10]. Over the past decades, HDACs have been validated as practical targets for cancer treatments[11].

Until now, 18 HDAC isoforms have been found in humans and can be divided into classes I, II, III and IV. Classes I (1, 2, 3, 8), II (4, 5, 6, 7, 9, 10) and IV (11) HDACs are Zn^{2+}-dependent enzymes, while class III HDACs (SIRT1−7) require NAD+ for their activities[12]. Recent development of HDAC inhibitors (HDACis) mainly focuses on Zn^{2+}-dependent HDACs. So far, five HDACis (SAHA[13], FK-228[14], PXD-101[15], LBH-589[16] and Chidamide[17]) (Figure 1) have been approved by the US FDA for the treatment of cutaneous T-cell lymphoma (CTCL),

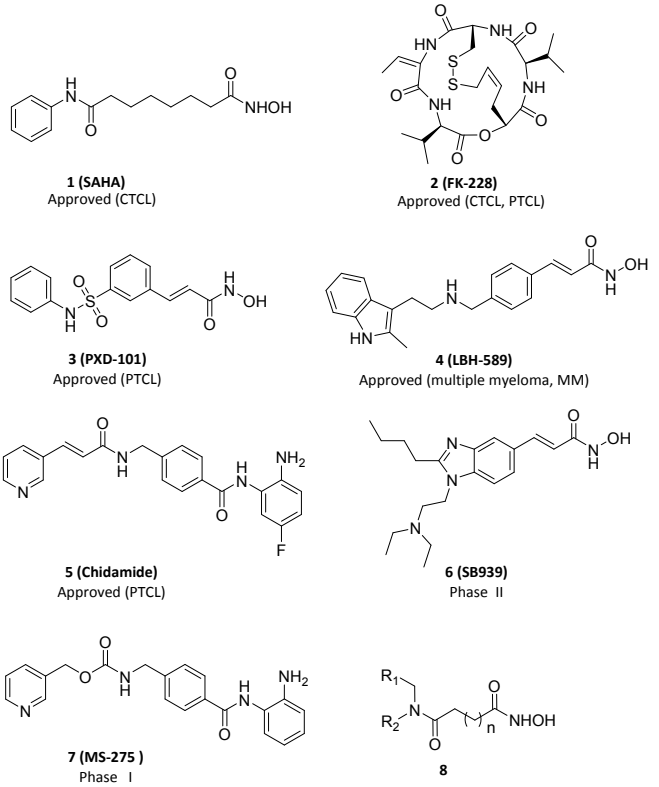

Fig. 1 HDAC inhibitors approved or under clinical development.

peripheral T-cell lymphoma (PTCL) or multiple myeloma (MM). A number of other inhibitors, such as **6** and **7**, are also processing at different stages of clinical investigations[11,17,18].

Structures of most common HDACis usually comprise three parts: a zinc binding group (ZBG), a linker and a surface

[a.] [1]*School of biological science and technology, University of Jinan, Jinan, Shandong Province 250022, China*
[b.] [2]*Shanghai Key Laboratory of Regulatory Biology, The Institute of Biomedical Sciences and School of Life Sciences, East China Normal University, Shanghai, 200241, China.*
[c.] **Corresponding Authors: Dr. Yihua Chen or Dr. Hua Zhang or Dr. Feifei Yang, E-mail: yhchen@bio.ecnu.edu.cn or bio_zhangh@ujn.edu.cn or yee68511@126.com.*
[d.] *# These authors contribute equally to this research work.*

recognition group (CAP group)[19,20]. Recent structural modifications of HDACis mainly focused on the CAP and linker moieties to develop novel molecules with optimized activities and selectivities[21,22]. In our previous study, we designed and synthesized a series of bis-substituted aromatic amide based hydroxamic acid HDACis[23], among which, compound **8a** displayed mild inhibition against nuclear extract HDAC. In this report, we aimed to seek more bis-substituted aromatic amides HDACis with better affinity and physicochemical properties based on the scaffold of **8a** as shown in Fig. 2. According to the preliminary results of docking studies of **8a** with HDAC1, we found that the *meta*-bromine in the A ring of CAP region was in the cavity of the rim of HDAC enzyme, so we replaced the bromine with different amides which could better occupy the cavity and a panel of new HDACis were synthesized and explored. Biological evaluations were also subsequently performed to examine their mechanism of action and *in vitro* antiproliferative activities in multiple cancer cell lines.

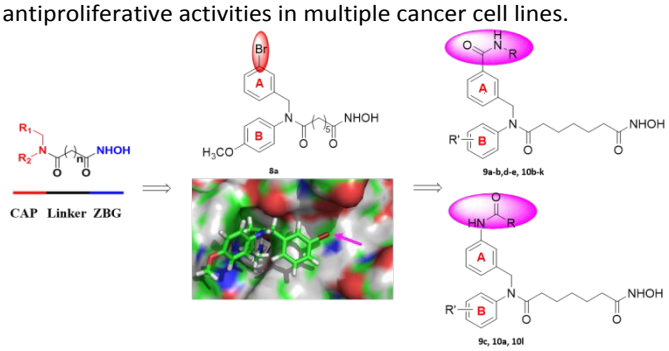

Fig. 2 Design strategy and general structures of the target compounds.

2. Results and discussion

2.1 Chemistry

The synthetic routes for compounds **9a**-**b**, **9d**-**e** and **10b**-**k** were depicted in Scheme 1. Compound **12** was coupled with different substituted amines in the presence of EDC and HOBt to generate **13a**-**k**. The intermediates **14a**-**n** were constructed from substituted anilines with **13a**-**k** through reductive amination and were further condensed with pimelic acid anhydride in 1,4-dioxane to yield acids **15a**-**n**. Subsequent esterification of **15a**-**n** in methanol with catalytic amount of thionyl chloride generated the corresponding esters **16a**-**n**, which were at last stirred with the freshly prepared hydroxylamine in methanol to afford hydroxamic acids **9a**-**b**, **9d**-**e** and **10b**-**k**.

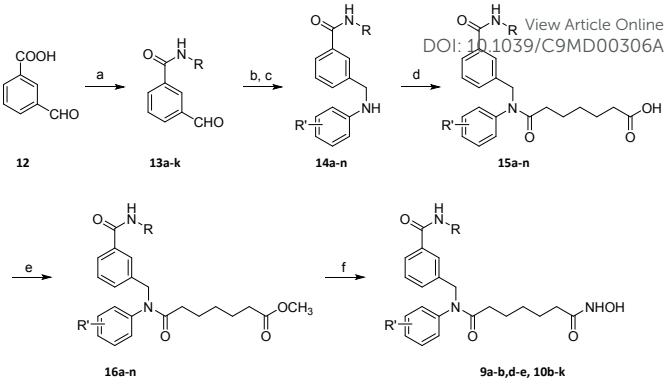

Scheme 1 Reagents and conditions: (a) RNH_2, EDC, HOBt, DMF; (b) $ArNH_2$, EtOH, 0 °C then to rt; (c) $NaBH_4$, 0 °C then to rt; (d) Anhydride, 1,4-dioxane, reflux; (e) MeOH, *Cat.* $SOCl_2$, reflux; (f) NH_2OH•HCl, KOH, MeOH.

The synthetic routes to compounds **9c**, **10a** and **10l** were illustrated in Scheme 2. The important intermediate **20a-b** were first synthesized via a similar procedure as **15a**-**n** in Scheme 1. Compound **21a-b** were then obtained after reduction of the nitro group of **20** and was further reacted with different substituted carboxylic acids to furnish **22a**-**c** containing the extra amide functionality. Finally, treatment of esters **22a**-**c** with hydroxylamine gave the desired hydroxamic acid derivatives **9c**, **10a** and **10l**.

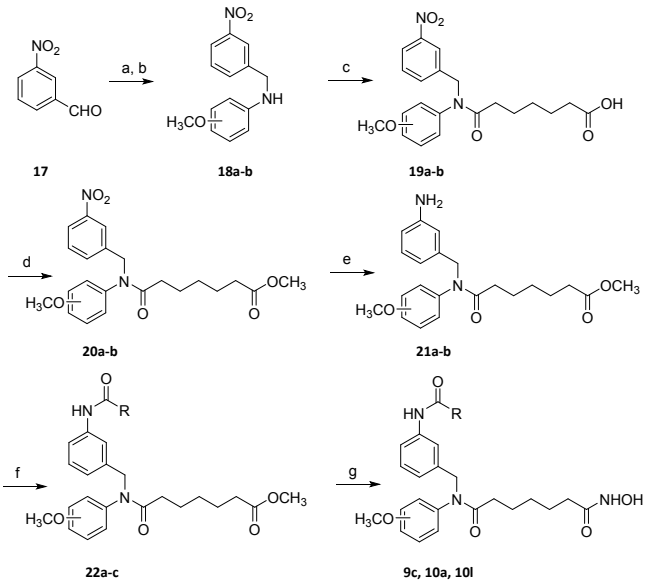

Scheme 2 Reagents and conditions: (a) *O*-anisidine, EtOH, 0 °C then to rt; (b) $NaBH_4$, 0 °C then to rt; (c) Anhydride, 1,4-dioxane, reflux; (d) MeOH, *Cat.* $SOCl_2$, reflux; (e) Zn, CH_3COOH, $EtOH/H_2O$; (f) RCOOH, EDC, HOBt, DMF; (g) NH_2OH•HCl, KOH, MeOH.

2.2 HDAC Inhibition Assay

Initially, the effect of amide group at meta-position of A ring was explored, compounds **9a-c** and **10a-j** with an arylalkyl amino carbonyl group at the meta-position of A ring and methoxy group at the ortho-position of B ring were assayed against nuclear extract HDAC (mainly contain HDAC1 and 2) with **1** (SAHA) as a reference drug. The assay results were

shown as inhibition rates as listed in Table 1. Compounds with mono-substitution and di-substitution on the nitrogen of amide (**9a-9b**) showed mild inhibitory activities. Excitingly, when a phenyl group was inserted to the terminal alkyl, most **10**-series compounds (**10a-c, 10g-h** and **10j**) exhibited better activities than the **9**-series. In addition, the inversion of the amide bond seemed to show little influence to the HDAC inhibition (**9a** *vs* **9c** and **10a** *vs* **10b**). Thus, the amide bond was retained in subsequent structural modifications. Analysis of compounds (**10b-f**) indicated that carbon chain length between nitrogen and benzene ring greatly affected the inhibitory potency. Compounds **10b** and **10c** containing one or two methylene bridge showed better activities than their analogues with longer linker (**10d-f**). Furthermore, introduction of electron-withdrawing groups to the terminal phenyl ring was beneficial for maintaining the inhibitory activities (**10g** & **10h** *vs* **10i**). Especially for the fluorine atom, compound **10j** also displayed much better activity than **10d**. Meanwhile, in consideration of the physicochemical properties of target compounds, LogP values of these derivatives were predicted through the ALOGPS 2.1 program (http://146.107.217.178/lab/alogps/start.html). As shown in Table 1, reports suggest that compounds with LogP between 1 and 3 could have good oral bioavailability[24]. The results heralded that compound **9a** may have the optimal absorption properties in this test.

Table 1 Inhibitory activity of compounds **9a**-**c** and **10a**-**j** on HDAC nuclear extract at 0.5 μM.

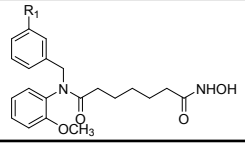

Compd.	R_1	Inhibition%	LogP
8a	Br-	21%	4.05
9a	CH_3CH_2NHCO-	20%	2.75
9b	$(CH_3CH_2)_2NCO$-	20%	3.44
9c	CH_3CH_2CONH-	22%	3.18
10a	$PhCH_2CONH$-	37%	3.98
10b	$PhCH_2NHCO$-	38%	3.74
10c	$Ph(CH_2)_2NHCO$-	38%	4.21
10d	$Ph(CH_2)_4NHCO$-	15%	5.06
10e	$Ph(CH_2)_5NHCO$-	16%	5.60
10f	$Ph(CH_2)_6NHCO$-	4%	6.07
10g	4-F-$Ph(CH_2)_2NHCO$-	39%	4.12
10h	4-Cl-$Ph(CH_2)_2NHCO$-	36%	4.71
10i	4-$OCH_3Ph(CH_2)_2NHCO$-	27%	4.47
10j	4-F-$Ph(CH_2)_4NHCO$-	34%	5.12
SAHA	--	46%	1.88

According to the results of our previous study, compounds with electron-donating groups at *para*-position of B ring appeared to be optimal for increasing activity.[23] Therefore, in light of physicochemical properties and the aforementioned activity results derived from the substituent exploration of A ring, two compounds (**9d** and **10k**) were further synthesized and evaluated, and a dramatic increase of potency was observed for both compounds, which could further confirm the conclusion that compounds with *para*-substituents are superior to the corresponding *ortho*-position derivatives. However, when the methoxyl of **9d** was replaced with hydroxyl, the resulting compound **9e** exhibited a decrease in inhibitory activity, which testified the importance of methoxy group for inhibitors. Meantime, compound **10l**, the "inverse amide" version of amide **10k**, exhibited slightly decreased activity.

Table 2 Inhibitory activity of compounds **9d-e** and **10k** on HDAC nuclear extract at 0.5 μM.

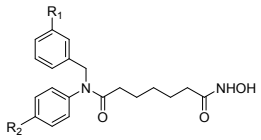

Compd.	R_1	R_2	Inhibition%	LogP
9d	CH_3CH_2NHCO-	4′-OCH_3	51%	2.85
9e	CH_3CH_2NHCO-	4′-OH	21%	2.53
10k	4-F-$Ph(CH_2)_2NHCO$-	4′-OCH_3	53%	4.16
10l	4-F-$Ph(CH_2)_2CONH$-	4′-OCH_3	49%	4.52
SAHA	-	-	46%	1.88

Next, **9d** and **10k** with the best nuclear extract HDAC inhibitory rates were further evaluated against HDAC1. Results (Table 3) revealed that the two compounds showed significant HDAC1 inhibitory activities, being >10 fold potent than SAHA.

Table 3 Inhibition activity of tested compounds on HDAC1.

Compd.	IC_{50} (nM)
9d	2.2±0.13
10k	2.3±0.16
SAHA	25.0±1.23

The data were expressed as the mean ± SD of three independent experiments.

The *in vitro* anti-proliferative activities of **9d** and **10k** against three human tumor cell lines MDA-MB-231, MCF-7 and A549 were then evaluated using the SRB assay. As shown in Table 4, it was found that A549 cells were more sensitive to compounds **9d** and **10k**, as compared to the reference drug SAHA. Compound **9d** showed the strongest growth inhibition toward A549 cells with an IC_{50} value of 2.13 μM close to that (2.93 μM) of SAHA.

Table 4 Anti-proliferative activities of representative compounds against tumor cells[a].

Compd.	IC_{50} (μM)		
	MDA-MB-231	MCF-7	A549
9d	6.87±0.84	6.96±0.84	2.13±0.33
10k	7.24±0.87	7.17±0.86	4.05±0.61
SAHA	4.66±0.67	6.17±0.56	2.93±0.47

[a] The inhibitory effects of individual compounds on the proliferation of cancer cell lines were determined by the SRB assay. The data were expressed as the mean ± SD of three independent experiments.

Moreover, to evaluate whether target compounds **9d** and **10k** show selectivity between cancer and non-cancer cells, the *in vitro* cytotoxicity of them was further tested against three normal cell lines: human breast epithelial cells (MCF-10A, MCF-10F) and human lung epithelial cells (Beas-2B). As shown in Table 5, the results indicated that both compounds displayed no obvious toxicities against the three human normal cells, and compound **9d** behaved even better than SAHA.

Table 5 Anti-proliferative activities of representative compounds against normal cells.

Compd.	IC_{50} (μM)		
	MCF-10A	MCF-10F	Beas-2B
9d	>100	>100	>100
10k	>50	>50	>20
SAHA	>50	>50	>50

2.3 Colony formation assay

Since compound **9d** showed the best antiproliferative activity against A549 cancer cell line among the investigated ones, we further evaluated its inhibitory behavior via colony formation assay, with SAHA as the positive control. As depicted in Figure 3, compound **9d** resulted in a significant inhibition of the colony formation more potently than SAHA. The results suggested that **9d** could at least partly inhibit the growth and development of A549 cells.

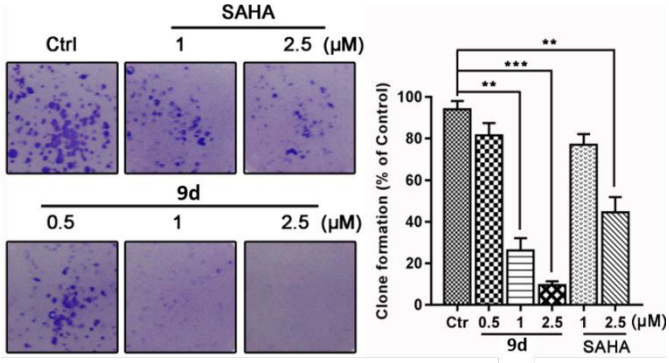

Fig. 3 Compound **9d** inhibited the colony formation of A549 cells. After treatment with different concentrations of **9d** and SAHA in 6-well plates for 7 days, cells were fixed with methanol and stained with 1% crystal violet and the number of cell clones were counted. Experiments were carried out in triplicate and repeated three times. Representative photographs from three independent experiments are shown. The data were expressed as means ± SD of three separate experiments. p values are for one-way analysis of variance (ANOVA). **p < 0.01, ***p < 0.001 vs control.

2.4 Anti-migration activity

Investigating the effect of novel HDAC inhibitors against cancer cell migration is valuable for the treatment of metastatic or advanced cancers. Based on the previous results that the bis-substituted aromatic amides showed potent activities against tumor cell migration [23], compound **9d** was then evaluated its anti-metastatic effects via wound-healing migration assay. As depicted in Figure 4, **9d** could decrease the migration of A549 cells in a dose-dependent manner, with higher potency than SAHA.

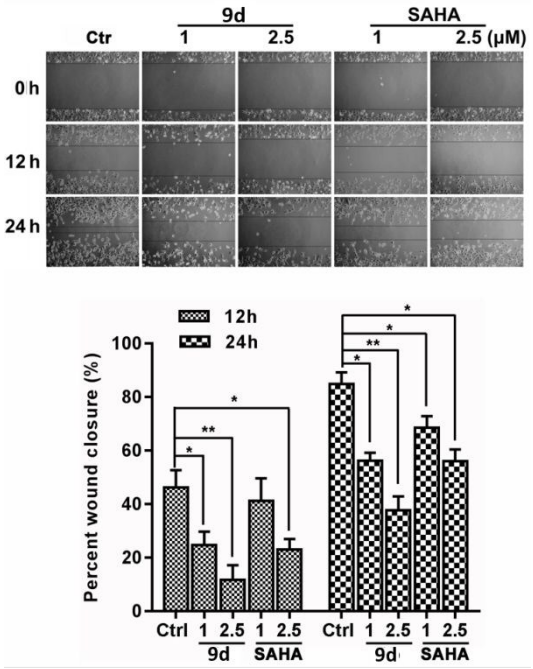

Fig. 4 Compound **9d** inhibited the wound healing of A549 cell lines. After a wound was made, cells were treated with different concentrations of **9d** and SAHA for 24 h. Representative photographs from three independent experiments are shown. The data were expressed as means ± SD of three separate experiments. p values are for one-way analysis of variance (ANOVA). *p < 0.05, **p < 0.01 vs control.

2.5 Western blot analysis

Considering the remarkable HDAC1 inhibitory potency, compound **9d** was progressed to western blot analysis by immunoblotting assay. A549 cells were incubated with SAHA and compound **9d** (1.0, 2.5 and 5.0 μM). As shown in Figure 5, **9d** could dramatically increase the levels of both acetyl-histone H3 and H4 in a dose-dependent manner, which was consistent with its HDAC1 inhibition activity. Compound **9d** displayed more potent activity to induce histone acetylation than SAHA.

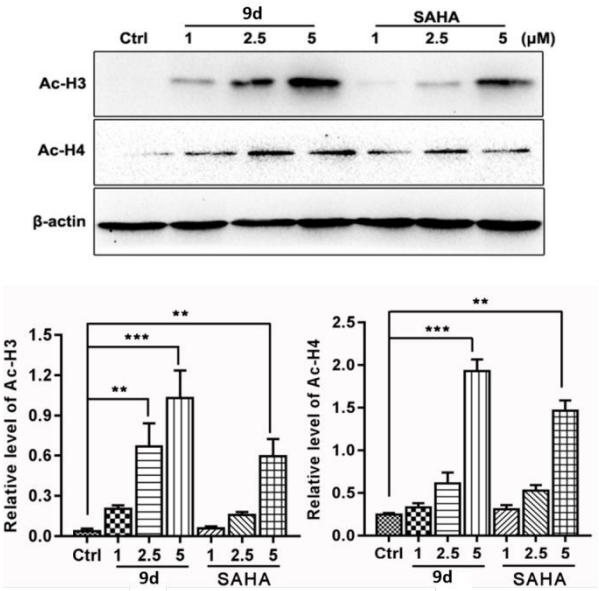

Fig. 5 Western blot analysis of **9d** on the effects of acetylated histone levels in A549 cancer cells. A549 cells were treated with different concentrations of **9d** or SAHA for 24 h. Cell lystates were lysed, collected and immunoblotted using western blotting. The relative levels of each protein compared to control β-actin were determined by densimetric scanning. Representative photographs from three independent experiments are shown. The data were expressed as means ± SD of three separate experiments. p values are for one-way analysis of variance (ANOVA). **p < 0.01, ***p < 0.001 vs control.

2.6. Cell cycle analysis

Cell cycle analysis of the most potent HDACi **9d** was investigated in A549 cancer cells. As shown in Fig. 6, in comparison to the control group, compound **9d** arrested A549 cells mainly in G2/M phase (40.3% at 5 μM for **9d**), which was obviously more potent than SAHA (24.97% at 5 μM). We also evaluated the effect of **9d** treatment on cell-cycle–regulatory proteins, CDK1 and cyclin B, which were involved in G2–M transition[25]. The results in Fig. 6 displayed that **9d** treatment decreased CDK1 and cyclin B1 protein levels.

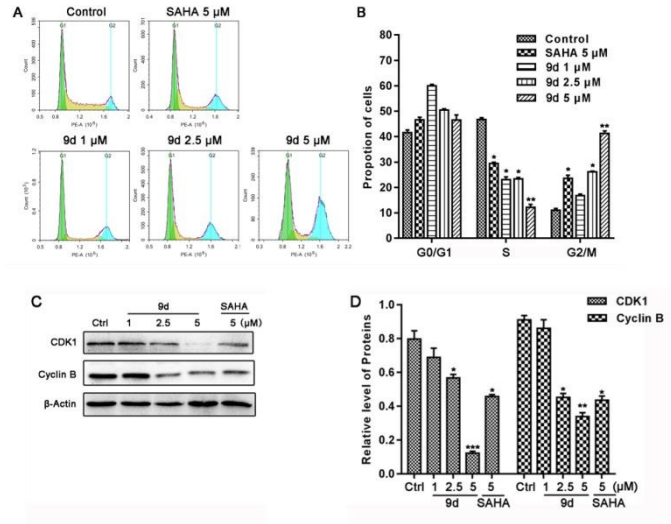

Fig. 6 The effects of **9d** on cell cycle progression in A549 cells. (A) A549 cells were treated with vehicle (control), SAHA, or different doses of **9d** and stained with PI, followed by flow cytometry analysis. Representative photographs from three independent experiments were shown. (B) Representative histograms. Data are expressed as means ± SD of the percentages of A549 cells from three independent experiments. p values are for one-way analysis of variance (ANOVA). *P < 0.05, **p < 0.01, ***p < 0.001 vs control. (C) The whole cell lysates were analyzed for the detection of cyclin B and CDK1 using western blot. β-Actin was used as an equal loading control. Representative photographs from three independent experiments were shown. (D) Quantitative analysis. The relative levels of CDK1 and Cyclin B used to control β-Actin were determined by densimetric scanning. The data are expressed as means ± SD of three separate experiments. p values are for one-way analysis of variance (ANOVA).*P < 0.05, **p < 0.01, ***p < 0.001 vs control. The blots are representative of three independent experiments

2.7 Cell apoptosis analysis

To further determine whether the antiproliferative effects of compound **9d** was associated with enhanced apoptosis of cancer cells, we carried out Annexin V-PE/7-AAD staining and flow cytometry assay, and the percentages of apoptotic cells were determined. A549 cancer cells were incubated with different concentrations of **9d** or SAHA for 72 h. As shown in Fig. 7, **9d** treated A549 cells exhibited a dose-dependent increase of apoptosis by 30.03%, 56.44%, and 81.45% at 1.0 μM, 2.5 μM, and 5.0 μM, respectively. The 81.45% induction of A549 cells apoptosis with 5.0 μM **9d** was higher than 5.0 μM SAHA (75.64% apoptotic cells). We also examined the cleavage states of caspase-3 and PARP (Fig. 7C and D). It was revealed that **9d** resulted in more cleavage of both PARP and caspase-3 the SAHA treated group. Taken together, these results proved that **9d** treatment induced apoptosis associated with cleavage of caspase 3 and PARP in A549 cells.

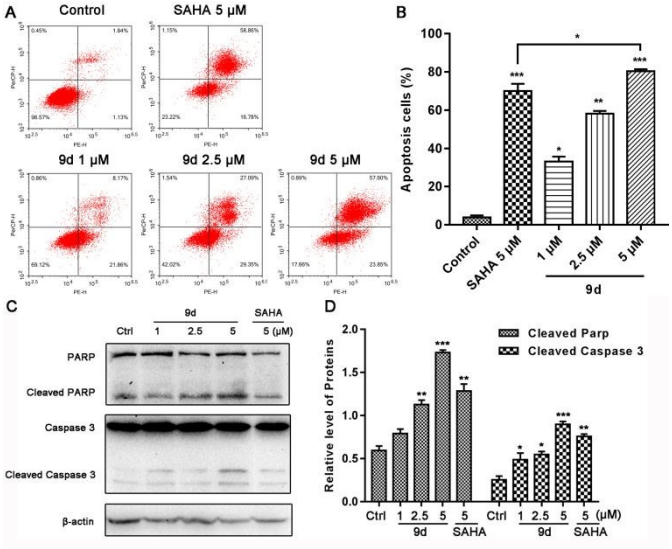

Fig. 7 The effects of **9d** on cell apoptosis in A549 cells. (A) Flow cytometry analysis. Representative photographs from three independent experiments were shown. (B) Quantitative analysis of apoptotic cells. Data are expressed as means ± S.D. of the percentages of apoptotic cells from three independent experiments. p values are for one-way analysis of variance (ANOVA). *P < 0.05, **p < 0.01, ***p < 0.001 vs control. (C) A549 cells were incubated with, or without, **9d** and SAHA at the indicated concentrations for 48 h and the levels of protein expression were detected using specific antibodies. Data shown are representative images of each protein for three separate experiments. (D) Quantitative analysis of cleaved caspase 3, and cleaved PARP. The relative levels of each protein compared to control β-actin were determined by densimetric scanning. Data are expressed as means ± SD from three separate experiments. p values are for

one-way analysis of variance (ANOVA). *P < 0.05, **p < 0.01, ***p < 0.001 vs control. The blots are representative of three independent experiments

2.8 Docking studies

Docking simulation was performed for the selected compound **9d** which was docked into HDAC1. Besides chelating with Zn^{2+}, the hydroxamic acid group of **9d** formed two hydrogen bonds with His140 and His178, respectively (Figure 8). Moreover, hydrogen bonding interaction was also observed between the amide group of **9d** and Leu271. In addition, the para-methoxy group of **9d** docked into the hydrophobic pocket of the surface region of HDAC1, which could preliminarily explain the better inhibitory activity of **9d** than other analogues.

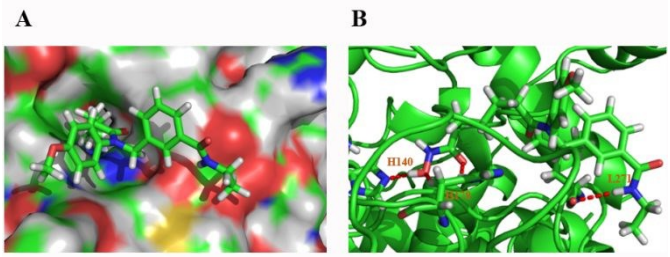

Fig. 8 Proposed binding mode of compound **9d** with HDAC1 (PDB 4BKX). (A) Molecular surface of the HDAC1 binding pocket with **9d**. (B) **9d** interacted with the active site of HDAC1.

3. Conclusion

In conclusion, a series of new bis-substituted aromatic amide based hydroxamic acid HDACis were designed, synthesized and evaluated for their antitumor activities. Two analogues **9d** and **10k** exhibited improved potency against HDAC1 compared with SAHA. Moreover, compound **9d** showed modest *in vitro* antiproliferative effects towards three different types of cancer cells, and increased the levels of acetylated histone H3 and H4 in dose dependent manner in A549 cells. Finally, molecular modeling study was also performed to assess the potential binding ability of **9d** to HDAC1. The present work afforded new HDACis that could be further investigated as promising anticancer drug leads.

4. Experimental section

4.1. Chemistry: general methods

All Reagents and solvents were purchased from Adamas-beta Ltd., Aladdin-reagents Inc., or J&K Inc., and used without further purification. All reactions were carried out using standard techniques and were monitored by TLC. ^{1}H and ^{13}C NMR spectra were recorded on Bruker 300 or 600 MHz instruments. The chemical shifts (δ) were reported in parts per million (ppm) and coupling constants (*J*) were reported in Hz. High resolution mass spectra were measured by Bruker MicroTOF-Q II LCMS instrument operating in electrospray ionization (ESI) mode. HPLC analyses were carried out on Agilent Technologies 1260 Series, using the following condition: Eclipse XDB C18 column, 5 μm, 4.6×150 mm, column temperature 40 °C; solvent A: water; solvent B: methanol; gradient of 40−70% B (0−5 min), 70−90% B (5−10 min), 90−40% B (10−15 min); flow rate of 1.5 mL/min. Purities of all compounds for biological test were ≥95%.

4.2. General procedure for the preparation of target compounds

4.2.1 N^1-(3-(ethylcarbamoyl)benzyl)-N^7-hydroxy-N^1-(2-methoxyphenyl) heptanediamide (9a)

To a solution of hydroxyl amine hydrochloride (945 mg, 13.6 mmol) in 10 mL MeOH was added KOH (763 mg, 13.6 mmol). Then the reaction mixture was stirred at 40 °C for 10 min and cooled to 0 °C and filtered. Compound methyl 7-((3-(ethylcarbamoyl)benzyl)(2-methoxyphenyl) amino)-7-oxoheptanoate (300 mg, 0.68 mmol) was added to the filtrate followed by KOH (76.3 mg, 1.36 mmol) at room temperature for 30 min. The solvent was removed and extracted with EtOAc. The organic layer was washed with saturated NH_4Cl aqueous solution and brine and dried over Na_2SO_4. The obtained residue was finally purified by column chromatography [eluted with EtOAc followed by 10:1 CH_2Cl_2-MeOH] to give compound **9a** as a colorless oil (179 mg, 59.5% yield).

^{1}H NMR (600 MHz, CD_3OD) δ 7.67 – 7.65 (m, 2H), 7.35 - 7.31 (m, 3H), 7.06 (d, *J* = 8.4 Hz, 1H), 6.94 (d, *J* = 7.8 Hz, 1H), 6.88 (dd, *J* = 7.8, 7.8 Hz, 1H), 5.15 (d, *J* = 14.4 Hz, 1H), 4.54 (d, *J* = 14.4 Hz, 1H), 3.74 (s, 3H), 3.38 (q, *J* = 7.2 Hz, 2H), 2.11 – 2.04 (m, 2H), 2.03 (d, *J* = 7.2 Hz, 2H), 1.57 – 1.54 (m, 2H), 1.52 – 1.49 (m, 2H), 1.25 – 1.22 (m, 2H), 1.21 (t, *J* = 7.2 Hz, 3H). ^{13}C NMR (150 MHz, CD_3OD) δ 176.15, 172.81, 169.84, 156.45, 139.27, 135.85, 133.01, 131.34, 131.14, 131.00, 129.38, 128.72, 127.15, 121.98, 113.38, 56.08, 52.75, 35.82, 34.46, 33.55, 29.60, 26.38, 25.96, 14.90. HRMS (ESI) m/z calcd for $C_{24}H_{31}N_3O_5$ $[M + H]^+$ 442.2336, found 442.2331. HPLC purity: 95.2%, t_R = 4.7 min.

4.2.2 N^1-(3-(diethylcarbamoyl)benzyl)-N^7-hydroxy-N^1-(2-methoxyphenyl) heptanediamide (9b)

Compound **9b** (35.9% yield) was prepared according to the procedure described for the preparation of compound **9a**. ^{1}H NMR (300 MHz, $CDCl_3$) δ 10.33 (brs, 1H), 7.43 (s, 1H), 7.27 – 7.22 (m, 3H), 7.08 (d, J = 7.2 Hz, 1H), 6.90 (d, *J* = 8.4 Hz, 1H), 6.83 (dd, *J* = 8.4, 8.4 Hz, 1H), 6.74 (d, *J* = 8.4 Hz, 1H), 5.31 (d, *J* = 14.1 Hz, 1H), 4.28 (d, *J* = 14.1 Hz, 1H), 3.72 (s, 3H), 3.53 - 3.50 (m, 2H), 3.23 – 3.20 (m, 2H), 2.17 (t, *J* = 6.9 Hz, 2H), 2.02 (t, *J* = 6.9 Hz, 2H), 1.67 – 1.56 (s, 4H), 1.28 – 1.20 (s, 6H), 1.12 – 1.06 (m, 2H). ^{13}C NMR (150 MHz, CD_3OD) δ 176.05, 173.37, 172.79, 156.46, 139.44, 138.00, 131.26, 131.16, 131.13, 130.98, 129.65, 127.67, 126.33, 121.97, 113.42, 56.13, 52.60, 44.92, 40.85, 34.45, 33.54, 29.61, 26.37, 26.00, 14.41, 13.06. HRMS (ESI) m/z calcd for $C_{26}H_{35}N_3O_5$ [M + H]+ 470.2649, found 470.2647. HPLC purity: 95.4%, t_R = 6.0 min.

4.2.3 N^1-(3-(propionamido)benzyl)-N^7-hydroxy-N^1-(2-methoxyphenyl)heptanediamide (9c)

Compound **9c** (16.6% yield) was prepared according to the procedure described for the preparation of compound **9a**. ^{1}H NMR (300 MHz, DMSO-*d6*): δ 10.30 (br s, 1H), 9.81 (br s, 1H), 8.65 – 8.62 (m, 1H), 7.51 (d, *J* = 8.1 Hz, 1H), 7.40 (s, 1H), 7.33 (dd, *J* = 7. 5, 7. 2 Hz, 1H), 7.17 – 7.10 (m, 2H), 6.98 (d, *J* = 7. 5 Hz, 1H), 6. 87 (dd, *J* = 7. 5, 7. 2 Hz, 1H), 6.77 (d, *J* = 7. 2 Hz, 1H), 5.20 (d, *J* = 14.1 Hz, 1H), 4.12 (d, *J* = 14.1Hz, 1H), 3.77 (s, 3H), 2.30 (q, *J* = 7.5 Hz, 2H), 1.87 (t, *J* = 7.2 Hz, 2H), 1.47 – 1.42 (m, 2H), 1.39 –1.34 (m, 2H), 1.20 – 1.15 (m, 4H), 1.08 (t, *J* = 7.5 Hz,

3H). ^{13}C NMR (150 MHz, CD_3OD) δ 176.02, 175.41, 172.82, 156.45, 139.96, 139.48, 131.43, 131.17, 131.04 , 129.58, 125.42, 121.88, 121.37, 120.12, 113.34, 56.13, 52.72, 34.45, 33.54, 31.02, 29.57, 26.36, 25.98, 10.28. HRMS (ESI) m/z calcd for $C_{24}H_{31}N_3O_5$ $[M + H]^+$ 442.2336, found 442.2330. HPLC purity: 99.2%, t_R = 5.2 min.

4.2.4 N^1-(3-(ethylcarbamoyl)benzyl)-N^7-hydroxy-N^1-(4-methoxy-phenyl) heptanediamide (9d)

Compound **9d** (49.1% yield) was prepared according to the procedure described for the preparation of compound **9a**. ^{1}H NMR (300 MHz, DMSO-d_6) δ 10.31 (brs, 1H), 8.65 (brs, 1H), 8.43 (t, *J* = 5.1 Hz), 7.68 (d, *J* = 7.5 Hz, 1H), 7.63 (s, 1H), 7.36 (dd, *J* = 7. 5, 7.5 Hz, 1H), 9.29 (d, *J* = 7.5 Hz, 1H), 7.04 (d, *J* = 8.7 Hz, 2H), 6.89 (d, *J* = 8.7 Hz, 2H), 4.85 (s, 2H), 3.72 (s, 3H), 3.26 (q, *J* = 7.2 Hz, 2H), 2.05 (t, *J* = 7.5 Hz, 2H), 1.89 (t, *J* = 7.5 Hz, 2H), 1.50 – 1.45 (m, 2H), 1.41 – 1.36 (m, 2H), 1.19 – 1.15 (m, 2H), 1.10 (t, *J* = 7.2 Hz, 3H). ^{13}C NMR (150 MHz, CD_3OD) δ 175.76, 172.81, 169.80, 160.86, 139.35, 136.10, 135.82, 132.78, 130.55, 129.66, 128.51, 127.22, 115.84, 55.94, 53.84, 35.84, 34.88, 33.54, 29.62, 26.37, 26.20, 14.89. HRMS (ESI) m/z calcd for $C_{24}H_{31}N_3O_5$ $[M + H]^+$ 442.2336, found 442.2342. HPLC purity: 99.1%, t_R = 4.6 min.

4.2.5 N^1-(3-(ethylcarbamoyl)benzyl)-N^7-hydroxy-N^1-(4-hydroxy-phenyl)heptanediamide (9e)

Compound **9e** (58.5% yield) was prepared according to the procedure described for the preparation of compound **9a**. ^{1}H NMR (600 MHz, CD_3OD) δ 7.69 (d, *J* = 7.2 Hz, 1H), 7.65 (s, 1H), 7.38 (dd, *J* = 7.8, 7.8 Hz, 1H), 7.34 (d, *J* = 7.8 Hz, 1H), 6.87 (d, *J* = 9.0 Hz, 2H), 6.74 (d, *J* = 9.0 Hz, 2H), 3.64 (s, 2H), 3.40 (q, *J* = 7.2 Hz, 2H), 2.14 (t, *J* = 7.8 Hz, 2H), 2.04 (d, *J* = 7.8 Hz, 2H), 1.60 – 1.57 (m, 2H), 1.54 – 1.51 (m, 2H), 1.27 – 1.24 (m, 2H), 1.21 (t, *J* = 7.2 Hz, 3H). ^{13}C NMR (150 MHz, CD_3OD) δ 175.89, 172.82, 170.06, 158.66, 139.41, 136.06, 134.69, 132.81, 130.48, 129.64, 128.50, 127.20, 117.15, 53.87, 52.08, 34.84, 33.54, 29.63, 26.39, 26.23, 14.88. HRMS (ESI) m/z calcd for $C_{23}H_{29}N_3O_5$ $[M + H]^+$ 428.2180, found 428.2177. HPLC purity: 95.6%, t_R = 4.4 min.

4.2.6 N^1-(3-(2-phenylacetamido)benzyl)-N^7-hydroxy-N^1-(2-methoxy-phenyl)heptanediamide (10a)

Compound **10a** (41.2% yield) was prepared according to the procedure described for the preparation of compound **9a**. ^{1}H NMR (300 MHz, DMSO-d_6): δ 10.31 (br s, 1H), 10.14 (br s, 1H), 8.66 (br s, 1H), 7.52 (d, *J* = 7. 2 Hz, 1H), 7.42 – 7.41 (m, 1H), 7.34 – 7.31 (m, 4H), 7.28 (d, *J* = 7. 2 Hz, 1H), 7.25 – 7.22 (m, 1H), 7.16 (dd, *J* = 7. 8, 7. 5 Hz, 1H), 7.10 (d, *J* = 7.5 Hz, 1H), 6.96 (d, *J* = 7.8 Hz, 1H), 6.88 (dd, *J* = 7. 5, 7. 5 Hz, 1H), 6.81 (d, *J* = 7.5 Hz, 1H), 5.21 (d, *J* = 14.7 Hz, 1H), 4.15 (d, *J* = 14.7 Hz, 1H), 3.75 (s, 3H), 3.62 (s, 2H), 1.95 – 1.90 (m, 2H), 1.87 (t, *J* = 7.5 Hz,, 2H), 1.45 (t, *J* = 7.5 Hz,, 2H), 1.37 (t, *J* = 7.5 Hz,, 2H), 1.12 - 1.08 (m, 2H). ^{13}C NMR (150 MHz, CD_3OD) δ 176.03, 172.82, 172.34, 156.43, 139.82, 139.50, 136.86, 131.40, 131.12, 131.02, 130.14, 129.98, 129.60, 127.95, 125.67, 121.89, 121.50, 120.23, 113.31, 56.09, 52.73, 44.70, 34.42, 33.52, 29.55, 26.34, 25.96. HRMS (ESI) m/z calcd for $C_{29}H_{33}N_3O_5$ $[M + H]^+$ 504.2493, found 504.2488. HPLC purity: 99.5%, t_R = 6.7 min.

4.2.7 N^1-(3-(benzylcarbamoyl)benzyl)-N^7-hydroxy-N^1-(2-methoxy-phenyl)heptanediamide (10b)

Compound **10b** (37.2% yield) was prepared according to the procedure described for the preparation of compound **9a**. ^{1}H NMR (600 MHz, CD_3OD) δ 7.73 – 7.69 (m, 1H), 7.68 (s, 1H), 7.35 – 7.34 (m, 2H), 7.33 – 7.29 (m, 5H), 7.26 – 7.24 (m, 1H), 7.04 (d, *J* = 7.8 Hz, 1H), 6.95 (d, *J* = 7.8 Hz, 1H), 6.88 (dd, *J* = 7.8, 7.8 Hz, 1H), 5.12 (d, *J* = 14.4 Hz, 1H), 4.57 (d, *J* = 14.4 Hz, 1H), 4.55 (s, 2H), 3.71 (s, 3H), 2.11 – 2.05 (m, 2H), 2.02 (t, *J* = 7.8 Hz, 2H), 1.57 – 1.52 (m, 2H), 1.51 – 1.48 (m, 2H), 1.24 – 1.20 (m, 2H). ^{13}C NMR (150 MHz, CD_3OD) δ 176.14, 172.80, 169.94, 156.44, 140.21, 139.29, 135.63, 133.20, 131.33, 131.13, 130.98, 129.54, 129.45, 128.84, 128.52, 128.19, 127.30, 121.99, 113.36, 56.06, 52.77, 44.48, 34.45, 33.54, 29.59, 26.37, 25.95. HRMS (ESI) m/z calcd for $C_{29}H_{33}N_3O_5$ $[M + H]^+$ 504.2493, found 504.2511. HPLC purity: 96.9%, t_R = 6.5 min.

4.2.8 N^1-hydroxy-N^7-(2-methoxyphenyl)-N^7-(3-(phenethyl-carbamoyl)benzyl) heptanediamide (10c)

Compound **10c** (35.6% yield) was prepared according to the procedure described for the preparation of compound **9a**. ^{1}H NMR (300 MHz, DMSO-d_6) δ 10.32 (s, 1H), 8.66 (s, 1H), 8.52 (t, *J* = 5.7 Hz, 1H), 7.64 (d, *J* = 8.7 Hz, 2H), 7.35 (d, *J* = 7.8 Hz, 2H), 7.31 – 7.28 (m, 2H), 7.24 (d, *J* = 9.0 Hz, 2H), 7.21 – 7.19 (m, 2H), 7.10 (d, *J* = 8.4 Hz, 1H), 6.94 (d, *J* = 7.5 Hz, 1H), 6.87 (dd, *J* = 7.5, 7.5 Hz, 1H), 5.17 (d, *J* = 14.7 Hz, 1H), 4.34 (d, *J* = 14.7 Hz, 1H), 3.74 (s, 3H), 3.49 – 3.43 (m, 2H), 2.82 (t, *J* = 7.5 Hz, 2H), 2.05 – 1.94 (m, 2H), 1.87 (t, *J* = 7.5 Hz, 2H), 1.48 – 1.41 (m, 2H), 1.39 – 1.33 (m, 2H), 1.13 – 1.07 (m, 2H). ^{13}C NMR (150 MHz, CD_3OD) δ 178.31, 176.63, 175.97, 172.82, 169.54, 161.12, 135.98, 133.80, 133.40, 130.70, 130.54, 130.37, 130.06, 128.91, 127.01, 126.84, 124.26, 116.14, 115.97, 56.00, 49.85, 46.27, 34.66, 34.46, 33.51, 29.53, 26.36, 26.00. HRMS (ESI) m/z calcd for $C_{30}H_{35}N_3O_5$ $[M + H]$+ 518.2649, found 518.2655. HPLC purity: 96.7%, t_R = 6.9 min.

4.2.9 N^1-hydroxy-N^7-(2-methoxyphenyl)-N^7-(3-((4-phenylbutyl) carbamoyl)benzyl)heptanediamide (10d)

Compound **10g** (34.6% yield) was prepared according to the procedure described for the preparation of compound **9a**. ^{1}H NMR (600 MHz, CD_3OD) δ 7.67 – 7.64 (m, 1H), 7.62 (s, 1H), 7.34 – 7.29 (m, 3H), 7.24 (dd, *J* = 7.8, 7.8 Hz, 2H), 7.18 (d, *J* = 7.2 Hz, 2H), 7.14 (dd, *J* = 7.2, 7.2 Hz, 1H), 7.03 (d, *J* = 8.4 Hz, 1H), 6.94 (d, *J* = 7.8 Hz, 1H), 6.87 (dd, *J* = 7.8, 7.8 Hz, 1H), 5.13 (d, *J* = 14.4 Hz, 1H), 4.55 (d, *J* = 14.4 Hz, 1H), 3.72 (s, 3H), 3.38 (t, *J* = 7.2 Hz, 2H), 2.66 (t, *J* = 7.2 Hz, 2H), 2.10 – 2.06 (m, 2H), 2.03 (t, *J* = 7.2 Hz, 2H), 1.70 – 1.67 (m, 2H), 1.65 – 1.61 (m, 2H), 1.56 – 1.53 (m, 2H), 1.52 – 1.49 (m, 2H), 1.24 – 1.19 (m, 2H). ^{13}C NMR (150 MHz, CD_3OD) δ 176.13, 172.81, 170.01, 156.45, 143.61, 139.24, 135.85, 133.04, 131.32, 131.13, 130.99, 129.45, 129.39, 129.33, 128.73, 127.18. 126.77, 121.98, 113.36, 56.08, 52.74, 40.76, 36.52, 34.46, 33.56, 30.08, 30.06, 29.60, 26.38, 25.96. HRMS (ESI) m/z calcd for $C_{32}H_{39}N_3O_5$ $[M + H]^+$ 546.2962, found 546.2972. HPLC purity: 96.1%, t_R = 7.8 min.

4.2.10 N^1-hydroxy-N^7-(2-methoxyphenyl)-N^7-(3-((5-phenylpentyl) carbamoyl)benzyl)heptanediamide (10e)

Compound **10e** (64.8% yield) was prepared according to the procedure described for the preparation of compound **9a**. ^{1}H NMR (600 MHz, CD_3OD) δ 7.65 – 7.63 (m, 1H), 7.62 (s, 1H), 7.36 – 7.30 (m, 3H), 7.22 (dd, *J* = 7.8, 7.2 Hz, 2H), 7.16 (d, *J* =

View Article Online
DOI: 10.1039/C9MD00306A

7.2 Hz, 2H), 7.12 (dd, *J* = 7.8, 7.2 Hz, 1H), 7.05 (dd, *J* = 8.4 Hz, 1H), 6.94 (d, *J* = 7.8 Hz, 1H), 6.88 (dd, *J* = 7.8, 7.8 Hz, 1H), 5.15 (d, *J* = 15.0 Hz, 1H), 4.54 (d, *J* = 15.0 Hz, 1H), 3.74 (s, 3H), 3.34 (t, *J* = 7.2 Hz, 2H), 2.62 (t, *J* = 7.8 Hz, 2H), 2.11 – 2.04 (m, 2H), 2.02 (t, *J* = 7.2 Hz, 2H), 1.69 – 1.64 (m, 2H), 1.63 – 1.60 (m, 2H), 1.58 – 1.55 (m, 2H), 1.52 – 1.48 (m, 2H), 1.42 – 1.37 (m, 2H), 1.24 – 1.20 (m, 2H). ^{13}C NMR (150 MHz, CD_3OD) δ 176.14, 172.78, 170.01, 156.46, 143.76, 139.26, 135.89, 133.00, 131.35, 131.14, 131.00, 129.43, 129.38, 129.27, 128.73, 127.17, 126.67, 121.98, 113.38, 56.09, 52.75, 40.91, 36.76, 34.47, 33.54, 32.37, 30.27, 29.60, 27.55, 26.38, 25.96. HRMS (ESI) m/z calcd for $C_{33}H_{41}N_3O_5$ [M + H]$^+$ 560.3119, found 560.3118. HPLC purity: 95.4%, t_R = 8.2 min.

4.2.11 *N*^{1}-hydroxy-*N*^{7}-(2-methoxyphenyl)-*N*^{7}-(3-((6-phenylhexyl)-carbamoyl)benzyl)heptanediamide (10f)

Compound **10j** (43.6% yield) was prepared according to the procedure described for the preparation of compound **9a**. ^{1}H NMR (300 MHz, DMSO-d_6): δ 10.31 (br s, 1H), 8.65 (br s, 1H), 8.37 (t, *J* = 5.1 Hz, 1H), 7.66 (d, *J* = 7.2 Hz, 1H), 7.62 (s, 1H), 7.32 (dd, *J* = 7.5, 7.5 Hz, 2H), 7.27 – 7.24 (m, 3H), 7.19 – 7.15 (m, 3H), 7.09 (d, *J* = 7. 2 Hz, 1H), 6.95 (d, *J* = 7.5 Hz, 1H), 6.87 (dd, *J* = 7.5, 7.5 Hz, 1H), 5.18 (d, *J* = 14.7 Hz, 1H), 4.35 (d, *J* = 14.7 Hz, 1H), 3.75 (s, 3H), 3.21 (q, *J* = 6.9 Hz, 2H), 2.59 (t, *J* = 7.8 Hz, 2H), 2.02 – 1.97 (m, 2H), 1.88 (t, *J* = 7.5 Hz, 2H), 1.55 (t, *J* = 7.8 Hz, 2H), 1.52 – 1.48 (m, 4H), 1.46 – 1.38 (m, 6H), 1.13 – 1.10 (m, 2H). ^{13}C NMR (151 MHz, CD_3OD) δ 176.14, 172.80, 170.00, 156.45, 143.90, 139.26, 135.89, 133.02, 131.33, 131.13, 130.99, 129.40, 129.26, 128.73, 127.22, 127.18, 126.64, 121.97, 113.37, 56.08, 52.74, 40.99, 36.83, 34.46, 33.55, 32.69, 30.42, 30.00, 29.60, 27.91, 26.37, 25.96. HRMS (ESI) m/z calcd for $C_{34}H_{43}N_3O_5$ [M + H]$^+$ 574.3275, found 574.3287. HPLC purity: 97.4%, t_R = 9.5 min.

4.2.12 *N*^{1}-(3-((4-fluorophenethyl)carbamoyl)benzyl)-*N*^{7}-hydroxy-*N*^{1}-(2-methoxyphenyl)heptanediamide (10g)

Compound **10g** (74.4% yield) was prepared according to the procedure described for the preparation of compound **9a**. ^{1}H NMR (300 MHz , DMSO-d_6): δ10.29 (br s, 1H), 8.63 (br s, 1H), 8.47 (t, *J* = 5.7 Hz, 1H), 7.64 – 7.61 (m, 2H), 7.32 (d, *J* = 7.5 Hz, 1H), 7.31 – 7.28 (m, 2H), 7.26 – 7.23 (m, 2H), 7.12 – 7.07 (m, 3H), 6.94 (d, *J* = 7.5 Hz, 1H), 6.87 (dd, *J* = 7.5, 7.5 Hz, 1H), 5.14 (d, *J* = 15.0 Hz, 1H), 4.33 (d, *J* = 15.0 Hz, 1H), 3.73 (s, 3H), 3.47 – 3.42 (m, 2H), 2.81 (t, *J* = 7.8 Hz, 2H), 2.02 – 1.97 (m, 2H), 1.87 (t, *J* = 7.2 Hz, 2H), 1.47 – 1.42 (m, 2H), 1.38 – 1.34 (m, 2H), 1.13 – 1.08 (m, 2H). ^{13}C NMR (150 MHz, CD_3OD) δ 176.14, 172.83, 170.01, 163.05 (d, *J* = 240.5 Hz), 156.46, 139.31, 136.55 (d, *J* = 3.3 Hz), 135.76, 133.11, 131.55 (d, *J* = 7.8 Hz), 131.33, 131.15, 130.99, 129.41, 128.70, 127.15, 121.99, 116.11 (d, *J* = 21.5 Hz), 113.39, 56.08, 52.73, 42.57, 35.67, 34.46, 33.56, 29.61, 26.38, 25.96. HRMS (ESI) m/z calcd for $C_{30}H_{34}FN_3O_5$ [M + H]$^+$ 536.2555, found 536.2563. HPLC purity: 96.6%, t_R = 6.9 min.

4.2.13 *N*^{1}-(3-((4-chlorophenethyl)carbamoyl)benzyl)-*N*^{7}-hydroxy-*N*^{1}-(2-methoxyphenyl)heptanediamide (10h)

Compound **10h** (62.5% yield) was prepared according to the procedure described for the preparation of compound **9a**. ^{1}H NMR (600 MHz, CD_3OD) δ 7.63 - 7.61 (m, 1H), 7.59 (s, 1H), 7.34 – 7.30 (m, 3H), 7.27 (d, *J* = 8.4 Hz, 2H), 7.24 (d, *J* = 8.4 Hz, 2H), 7.05 (d, *J* = 8.4 Hz, 1H), 6.93 (d, *J* = 7.8 Hz, 1H), 6.88 (dd, *J* = 8.4, 8.4 Hz, 1H), 5.13 (d, *J* = 14.4 Hz, 1H), 4.54 (d, *J* = 14.4 Hz, 1H), 3.72 (s, 3H), 3.56 (t, *J* = 7.8 Hz, 2H), 2.89 (t, *J* = 7.2 Hz, 2H), 2.13 – 2.04 (m, 2H), 2.03 (t, *J* = 7.2 Hz, 2H), 1.59 – 1.54 (m, 2H), 1.52 – 1.48 (m, 2H), 1.25 – 1.20 (m, 2H). ^{13}C NMR (150 MHz, CD_3OD) δ 176.12, 172.81, 170.04, 156.46, 139.44, 139.31, 135.72, 133.16, 133.12, 131.54, 131.32, 131.15, 130.98, 129.52, 129.41, 128.69, 127.16, 121.99, 113.39, 56.08, 52.72, 42.31, 35.80, 34.46, 33.56, 29.61, 26.38, 25.96. HRMS (ESI) m/z calcd for $C_{30}H_{34}ClN_3O_5$ [M + H]$^+$ 552.2260, found 552.2256. HPLC purity: 97.0%, t_R = 7.5 min.

4.2.14 *N*^{1}-hydroxy-*N*^{7}-(3-((4methoxyphenethyl)carbamoyl)benzyl)-*N*^{7}-(2-methoxyphenyl)heptanediamide (10i)

Compound **10i** (37.3% yield) was prepared according to the procedure described for the preparation of compound **9a**. ^{1}H NMR (600 MHz, CD_3OD) δ 7.63 – 7.62 (m, 1H), 7.60 (s, 1H), 7.34 – 7.32 (m, 3H), 7.15 (d, *J* = 9.0 Hz, 2H), 7.05 (d, *J* = 8.4 Hz, 1H), 6.94 (d, *J* = 7.8 Hz, 1H), 6.88 (dd, *J* = 7.8, 7.8 Hz, 1H), 6.84 (d, *J* = 8.4 Hz, 2H), 5.14 (d, *J* = 14.4 Hz, 1H), 4.54 (d, *J* = 14.4 Hz, 1H), 3.76 (s, 3H), 3.72 (s, 3H), 3.53 (t, *J* = 7.8 Hz, 2H), 2.83 (t, *J* = 7.2 Hz, 2H), 2.12 – 2.07 (m, 2H), 2.03 (t, *J* = 7.2 Hz, 2H), 1.58 – 1.55 (m, 2H), 1.53 – 1.50 (m, 2H), 1.25 – 1.20 (m, 2H). ^{13}C NMR (150 MHz, CD_3OD) δ 176.13, 172.80, 170.02, 159.76, 156.46, 139.28, 135.84, 133.06, 132.54, 131.33, 131.14, 130.99, 130.82, 129.39, 128.69, 127.16, 121.99, 114.92, 113.39, 56.08, 55.65, 52.73, 42.82, 35.66, 34.47, 33.56, 29.61, 26.39, 25.96. HRMS (ESI) m/z calcd for $C_{31}H_{37}N_3O_6$ [M + H]$^+$ 548.2755, found 548.2756. HPLC purity: 95.3%, t_R = 6.7 min.

4.2.15 *N*^{1}-(3-((4-(4-fluorophenyl)butyl)carbamoyl)benzyl)-*N*^{7}-hydroxy-*N*^{1}-(2-methoxyphenyl)heptanediamide (10j)

Compound **10j** (63.2% yield) was prepared according to the procedure described for the preparation of compound **9a**. ^{1}H NMR (300 MHz, DMSO-d_6): δ 10.30 (br s, 1H), 8.64 (br s, 1H), 8.39 (t, *J* = 5.1 Hz, 1H), 7.65 (d, *J* =6.9 Hz, 1H), 7.62 (s, 1H), 7.33 – 7.30 (m, 3H), 7.21 (dd, *J* = 7.5, 7.5 Hz, 2H), 7.10 – 7.06 (m, 3H), 6.94 (d, *J* = 7.5 Hz, 1H), 6.84 (dd, *J* = 7.5, 7.5 Hz, 1H), 5.15 (d, *J* = 14.7 Hz, 1H), 4.32 (d, *J* = 14.7 Hz, 1H), 3.73 (s, 3H), 3.25 (q, *J* = 7.2 Hz, 2H), 2.58 (t, *J* = 7.2 Hz, 2H), 2.10 – 1.97 (m, 2H), 1.87 (t, *J* = 7.2 Hz, 2H), 1.55 – 1.50 (m, 4H), 1.40 – 1.32 (m, 4H), 1.16 – 1.11 (m, 2H). ^{13}C NMR (150 MHz, CD_3OD) δ 176.14, 172.82, 170.02, 162.69 (d, *J* = 240.5 Hz), 156.45, 139.51 (d, *J* = 3.0 Hz), 139.27, 135.85, 133.04, 131.34, 131.14, 131.01 (d, *J* = 6.7 Hz), 129.41, 128.73, 127.71, 121.98, 115.84 (d, *J* = 21.0 Hz), 113.37, 56.08, 52.75, 40.71, 35.62, 34.46, 33.56, 30.11, 30.00, 29.60, 26.38, 25.96. HRMS (ESI) m/z calcd for $C_{32}H_{38}FN_3O_5$ [M + H]$^+$ 564.2868, found 564.2882. HPLC purity: 95.9%, t_R = 7.7 min.

4.2.16 *N*^{1}-(3-((4-fluorophenethyl)carbamoyl)benzyl)-*N*^{7}-hydroxy-*N*^{1}-(4-methoxyphenyl)heptanediamide (10k)

Compound **10k** (48.7% yield) was prepared according to the procedure described for the preparation of compound **9a**. ^{1}H NMR (300 MHz, DMSO-d_6): δ 10.33 (br s, 1H), 8.67 (br s, 1H), 8.53 (t, *J* = 5.4 Hz, 1H), 7.65 (d, *J* = 7. 5 Hz, 1H), 7.61 (s, 1H), 7.36 (dd, *J* = 7. 5, 7. 5 Hz, 1H), 7.31 – 7.23 (m, 3H), 7.10 (d, *J* = 9.0 Hz, 2H), 7.04 (d, *J* = 9.0 Hz, 2H), 6.89 (d, *J* = 8.7 Hz, 2H), 4.85 (s, 2H), 3.72 (s, 3H), 3.47 – 3.40 (m, 2H), 2.80 (t, *J* = 7.5 Hz, 2H), 2.03 (t, *J* = 7.2 Hz, 2H), 1.88 (t, *J* = 7.2 Hz, 2H), 1.49 – 1.45 (m,

2H), 1.40 – 1.35 (m, 2H), 1.12 – 1.09 (m, 2H). ^{13}C NMR (150 MHz, CD_3OD) δ 175.73, 172.43, 169.98, 163.03 (d, *J* = 241 Hz), 160.84, 139.38, 136.54 (d, *J* = 3.2 Hz), 136.00, 135.80, 132.86, 131.55 (d, *J* = 8.0 Hz), 130.54, 129.70, 128.45, 127.23, 116.05 (d, *J* = 21.2 Hz), 115.84, 55.94, 53.83, 42.60, 35.67, 34.88, 33.42, 29.62, 26.38, 26.20. HRMS (ESI) m/z calcd for $C_{30}H_{34}FN_3O_5$ $[M + H]^+$ 536.2555, found 536.2556. HPLC purity: 97.2%, t_R = 8.6 min.

4.2.17 N^1-(3-(3-(4-fluorophenyl)propanamido)benzyl)-N^7-hydroxy-N^1-(4-methoxyphenyl)heptanediamide (10l)

Compound **10l** (33.5% yield) was prepared according to the procedure described for the preparation of compound **9a**. ^{1}H NMR (600 MHz, DMSO-d_6) δ 10.31 (brs, 1H), 9.88 (s, 1H), 8.65 (brs, 1H), 7.49 (d, *J* = 8.4 Hz, 1H), 7.37 (s, 1H), 7.28-7.25 (m, 2H), 7.17 (dd, *J* = 7.8, 7.8 Hz, 1H), 7.09 (dd, *J* = 8.4, 8.4 Hz, 2H), 7.06 (d, *J* = 8.4 Hz, 2H), 6.90 (d, *J* = 8.4 Hz, 2H), 6.79 (d, *J* = 7.2 Hz, 1H), 4.75 (s, 2H), 3.73 (s, 3H), 2.88 (t, *J* = 7.8 Hz, 2H), 2.59 (t, *J* = 7.2 Hz, 2H), 2.01 (t, *J* = 7.2 Hz, 2H), 1.89 (t, *J* = 7.2 Hz, 2H), 1.49-1.44 (m, 2H), 1.40 -1.35 (m, 2H), 1.15 -1.01 (m, 2H). ^{13}C NMR (150 MHz, DMSO-d_6) δ 171.97, 170.27, 169.04, 160.69 (d, *J* = 239.8 Hz), 158.28, 139.19, 138.33, 137.31 (d, *J* = 3.0 Hz), 134.88, 130.02 (d, *J* = 7.8 Hz), 129.33, 128.59, 122.63, 118.38, 117.72, 114.96 (d, *J* = 20.8 Hz), 114.57, 55.24, 52.03, 38.00, 33.25, 32.13, 29.93, 28.21, 24.93, 24.68. HRMS (ESI) m/z calcd for $C_{30}H_{34}FN_3O_5$ $[M + H]^+$ 536.2555, found 536.2553. HPLC purity: 98.1%, t_R = 8.9 min.

4.3 HDAC1 inhibitory assay

The in vitro HDAC1 inhibitory activity was determined by the protease-coupled assay. Different concentrations of tested compounds were incubated with recombinant HDAC1 (BPS Biosciences, US) at room temperature for 15 min, followed by addition of trypsin as well as Ac-peptide-AMC substrates to initiate the reaction in Tris-based assay buffer. Fluorescent AMC released from substrate was measured on SynergyMx (BioTek, US) using filter sets as excitation = 355 nm and emission = 460 nm. IC50 values were calculated by GraphPad Prism software (California, USA).

4.4 Biological evaluation

4.4.1 *In vitro* anti-proliferation assay

Cell lines A549, MDA-MB-231, MCF-7 used in this study were obtained from the American Type Culture Collection. The cells were cultured in RPMI 1640 medium (HyClone, SH30809.01B) supplemented with 10% fetal bovine serum (FBS) (HyClone, SV30087.02) at 37 °C in a humidified atmosphere with 5% CO_2. Human breast epithelial cells (MCF-10A, MCF-10F) and human lung epithelial cells (Beas-2B) were obtained from the Type Culture Collection of the Chinese Academy of Sciences, Shanghai, China. And the cells were cultured in MEM (HyClone, SH30243.01B) supplemented with 10% fetal bovine serum (FBS) (Gibco, 10270) at 37 °C in a humidified atmosphere with 5% CO_2.

SRB assay was performed according to the manufacturer's instruction (Sigma Aldrich). Tumor cells were seeded into 96-well plates at the appropriate cell densities during the experiment. After incubation for 24 h, the cells were treated with various concentrations of tested compounds for 48 h. Then the cells were fixed with 10% TCA for 1 h at 4 °C and washed with distilled-water for five times. The plates were allowed to air drying followed by being dyed with 0.4% SRB for 5 min at room temperature. After dying, the plates were washed with 1% acetic acid and allowed to air drying. 150 μL of 10 mM Tris-based solution was added to each well, and the absorption at 540 nm was measured by microplate reader (TECAN). The IC50 was calculated using GraphPad prism 7.0. Three independent experiments were carried out in triplicate.

4.4.2 Colony formation assay

A549 cells were plated into 35 mm dishes (800 cells per dish) and treated with 9d or SAHA for one week and replenish every 24 h. After the removal of culture media, cells were washed with PBS for three times prior to methanol fixation. The cells were then immediately stained using 1% crystal violet (Beyotime) for 15 min and washed with PBS for one time. Images were collected using a scanning apparatus (Canon, Japan). Experiments were carried out in triplicate and repeated three times.

4.4.3 Wound healing assay

$1.5x10^5$ A549 cells were counted and plated in a 6-well dishes. Cells were incubated overnight yielding confluent monolayers for wounding. Wounds were made using a pipette tip and photographs taken immediately (0 h), 12 h and 24 h after wounding for A549 cells, respectively. The distance migrated by the cell monolayer to close the wounded area during this time period was measured via the Image J software (NIH, USA). Results were expressed as the percent of wound clousure—that is, the distance migrated 0 h minus the distance migrated 12 h or 24 h then relative to the distance migrated 0 h. Experiments were carried out in triplicate and repeated three times.

4.4.4 Western blotting

After treatment with 9d for indicated times, cells were harvested with RIPA buffer containing 150 mM sodium chloride, 1% Triton X-100, 0.5% sodium deoxycholate, 0.1% SDS, 50 mM Tris and cocktails of protease and phosphatase inhibitors for 10 min at room temperature and boiled for another 10 min. Equal amounts of total proteins (35 μg) underwent 15% SDS PAGE and were electroblotted onto the polyvinylidene difluoride (PVDF) membrane. The membrane was blocked with 5% (w/v) non-fat dry milk in PBS-Tween 20 (PBST; 0.05%) for 1 h and incubated with primary antibody (1:1000 in PBST) at 4 ℃ overnight. After three washings in PBST, the PVDF membrane was incubated with appropriate horseradish peroxidase-conjugated secondary antibodies (1:20000) for 1 h at room temperature. The immunoreactive bands were developed with the ECL western blotting system. β-actin were used as loading control. The relative quantity of proteins was analyzed via the Image J software (NIH, USA).

4.4.5 Cell cycle analysis

Cell cycle analysis was carried out by estimating DNA contents with flow cytometry. After incubation with the indicated doses of **9d** for 24 h, A549 cells were fixed in 70% ice-cold ethanol, incubated overnight at -20 °C, stained with PI containing RNaseA solution for 30 min at 37 °C, and then analyzed by FACS.

4.4.6 Cell apoptosis analysis

Cell apoptosis analysis was measured by annexin V FITC/PI assay using Annexin v-PE/7-AAD Apoptosis Detection kit (BD). Briefly, A549 cells (8 × 104/well) were treated with DMSO and compounds **9d** for 72 h. The cells were then harvested and stained with annexin binding buffer, Alexa Fluor 488 annexin and propidium iodide for 15 min in the dark. After staning, 400 uL of 1X annexin-building buffer was added, mixed gently and kept on ice. The samples were measured using an ACEA Biosciences novocyte flow cytometer.

4.5 Molecular docking studies

Molecular docking studies were carried out with Autodock-4.27. For the docking calculations HDAC1 crystal structure (PDB code: 4BKX) was retrieved from the Protein Data Bank (www.pdb.org). For protein preparation, all the water molecules were removed from HDAC1, and gasteiger partial charges were assigned to the selected compounds and enzyme atoms. The docking results were analyzed with the programs AutoDockTools, 27 DOCKRES and VMD.

4.6 Statistical analyses

All experiments were performed in duplicate and repeated at least three times. Each experimental value was expressed as the mean $\pm$ standard deviation (SD). Data were analyzed by

Student's t-test between two groups and by one-way analysis of variance (ANOVA) followed by Bonferroni test for multiple comparison. These analyses were performed using GraphPad Prism Software Version 5.0 (GraphPad Software, Inc. CA). *, ** and *** indicated $P < 0.05$, $P < 0.01$ and $P < 0.001$, respectively.

Conflicts of interest

The authors declare that there are no conflicts of interest.

Acknowledgements

This work was financially supported by the National Science Foundation of China (No. 81703360, 31501122, 81673304), Open Research Project Foundation of Shanghai Key Laboratory of Regulatory Biology (2018LBR03), the Natural Science Foundation of Shandong Province (No. ZR2016HB43, JQ2017021), Shandong Excellent Young Scientist Award Fund (BS2014SW031), the Young Taishan Scholars Program (tsqn20161037), and the Shandong Talents Team Cultivation Plan of University Preponderant Discipline (No. 10027).

Notes and references

1. M. Alzrigat, A. A. Parraga and H. Jernberg-Wiklund, *Semin. Cancer Biol.*, 2018, **51**, 101-115.
2. C. B. Yoo and P. A. Jones, *Nat. Rev. Drug Discov.*, 2006, **5**, 37-50.
3. S. Kotian, L. Zhang, M. Boufraqech, K. Gaskins, S. K. Gara, M. Quezado, N. Nilubol and E. Kebebew, *Clin. Cancer Res.*, 2017, **23**, 5044-5054.
4. Y. C. Tseng, S. K. Kulp, I. L. Lai, E. C. Hsu, W. A. He, D. E. Frankhouser, P. S. Yan, X. Mo, M. Bloomston, G. B. Lesinski, G. Marcucci, D. C. Guttridge, T. Bekaii-Saab and C. S. Chen, *J. Natl. Cancer Inst.*, 2015, **107**, djv274.
5. Y. Zhang, H. Fang, J. Jiao and W. Xu, *Curr. Med. Chem.*, 2008, **15**, 2840-2849.
6. M. A. Dawson and T. Kouzarides, *Cell*, 2012, **150**, 12-27.
7. A. M. A. Aboeldahab, E. A. M. Beshr, M. E. Shoman, S. M. Rabea and O. M. Aly, *Eur. J. Med. Chem.*, 2018, **146**, 79-92.
8. M. Haberland, R. L. Montgomery and E. N. Olson, *Nat. Rev. Genet.*, 2009, **10**, 32-42.
9. A. J. de Ruijter, A. H. van Gennip, H. N. Caron, S. Kemp and A. B. van Kuilenburg, *Biochem J.*, 2003, **370**, 737-749.
10. M. Mrakovcic, L. Bohner, M. Hanisch and L. F. Frohlich, *Int. J. Mol. Sci.*, 2018, **19**.
11. Y. Sun, F. Lu, Y. Sun, S. Yue and Y. Wang, *Curr. Top. Med. Chem.*, 2018, **18**, 2420-2428.
12. O. Khan and N. B. La Thangue, *Immunol. Cell Biol.*, 2012, **90**, 85-94.
13. P. A. Marks and R. Breslow, *Nat. Biotechnol.*, 2007, **25**, 84-90.
14. L. P. Yang, *Drugs*, 2011, **71**, 1469-1480.
15. R. M. Poole, *Drugs*, 2014, **74**, 1543-1554.
16. K. P. Garnock-Jones, *Drugs*, 2015, **75**, 695-704.
17. K. Stenzel, A. Hamacher, F. K. Hansen, C. G. W. Gertzen, J. Senger, V. Marquardt, L. Marek, M. Marek, C. Romier, M. Remke, M. Jung, H. Gohlke, M. U. Kassack and T. Kurz, *J. Med. Chem.*, 2017, **60**, 5334-5348.
18. Y. Luan, J. Li, J. A. Bernatchez and R. Li, *J. Med. Chem.*, 2019, **62**, 3171-3183.
19. J. E. Bolden, M. J. Peart and R. W. Johnstone, *Nat. Rev. Drug Discov.*, 2006, **5**, 769-784.
20. F. Thaler and C. Mercurio, *ChemMedChem*, 2014, **9**, 523-526.
21. W. Chen, G. Dong, Y. Wu, W. Zhang, C. Miao and C. Sheng, *ACS Med. Chem. Lett.*, 2018, **9**, 34-38.
22. M. Hassanzadeh, K. Bagherzadeh and M. Amanlou, *J. Mol. Graph. Model.*, 2016, **70**, 170-180.
23. F. Yang, T. Zhang, H. Wu, Y. Yang, N. Liu, A. Chen, Q. Li, J. Li, L. Qin, B. Jiang, X. Wang, X. Pang, Z. Yi, M. Liu and Y. Chen, *J. Med. Chem.*, 2014, **57**, 9357-9369.
24. D. F. Veber, S. R. Johnson, H.-Y. Cheng, B. R. Smith, K. W. Ward and K. D. Kopple, *J. Med. Chem.*, 2002, **45**, 2615-2623.
25. M. B. Kastan and J. Bartek, *Nature*, 2004, **432**, 316-323.